 CMC, vol.59, no.1, pp.105-118, 2019

# Lever Arm Compensation of Autonomous Underwater Vehicle for Fast Transfer Alignment

**Qi Wang[1, 2, *], Changsong Yang[1, 2], Shaoen Wu[3] and Yuxiang Wang[1, 2]**

**Abstract:** Transfer alignment is used to initialize SINS (Strapdown Inertial Navigation System) in motion. Lever-arm effect compensation is studied existing in an AUV (Autonomous Underwater Vehicle) before launched from the mother ship. The AUV is equipped with SINS, Doppler Velocity Log, depth sensor and other navigation sensors. The lever arm will cause large error on the transfer alignment between master inertial navigation system and slave inertial navigation system, especially in big ship situations. This paper presents a novel method that can effectively estimate and compensate the flexural lever arm between the main inertial navigation system mounted on the mother ship and the slave inertial navigation system equipped on the AUV. The nonlinear measurement equation of angular rate is derived based on three successive rotations of the body frame of the master inertial navigation system. Nonlinear filter is utilized as the nonlinear estimator for its capability of non-linear approximation. Observability analysis was conducted on the SINS state vector based on singular value decomposition method. State equation of SINS was adopted as the system state equation. Simulation experiments were conducted and results showed that the proposed method can estimate the flexural lever arm more accurately, the precision of transfer alignment was improved and alignment time was shortened accordingly.

**Keywords:** Transfer alignment, SINS, lever-arm effect, AUV, observability analysis.

## 1 Introduction

Transfer alignment is the process of initializing the position, velocity and attitude of a slave INS, using the data supplied by another INS known as the master inertial navigation system [John and Leondes (1972)]. As the initial attitude errors cause the navigation errors to increase much rapidly than the initial velocity and position errors [Cheng, Wang and Liu (2014)], thus the relative attitude error of the slave INS with respect to the master INS is a major error source to result in the position error growth after launching the inertial guided weapons [Zhu and Cheng (2013)]. A digital filter method was applied in compensating the lever arm effect [Xu and Wan (1994)]. Special attention has been paid

[1] School of Computer and software, Nanjing University of Information Science and Technology, Nanjing, 210044, China.

[2] Jiangsu Engineering Center of Network Monitoring, Nanjing University of Information Science and Technology, Nanjing, 210044, China.

[3] Department of Computer Science, Ball State University, Muncie 47306, USA.

[*] Corresponding Author: Qi Wang. Email: 002086@nuist.edu.cn.

to the estimation of the slave INS attitude estimation. In the case of shipborne slave INS, both the time taken to achieve an alignment and the accuracy which can be achieved are highly dependent on the angular motion of the ship, and there are still some difficulties in aligning slave INS with the mater reference [Kassas and Humphreys (2014)]. For example, the application of velocity matching [Sun, Xu and Liu (2016)] alone is greatly limited in the shipborne alignment because ships are unable to make such maneuver as an aircraft do. In addition, the dynamic state of different points [Zhu, Cheng and Wang (2016)]. The location of the slave INS is not usually equipped at the swaying center, resulting in a lever effect on the system, leading to an impact on the initial alignment. The optimal estimation theory [Li, Wang and Liu (2014)] was introduced in the master-slave inertial navigation system supposing the master inertial navigation system was already calibrated and initialized accurately. The velocity error between the master inertial navigation system and the slave inertial navigation system can be regarded as the measurements in the system. An angle rate matching method [Wang, Gu, Ma et al. (2017); Zhou, Wang, Wu et al. (2017)] was applied in estimating the angle error. The velocity vector projecting on the inertial frame differences can be used in the angle error between the two frames requiring the angle movement Butterworth filter was designed according to the real acceleration and the lever-arm acceleration distributed in the different frequency zones restraining the bad acceleration and compensating the lever arm effect [Chen, Chen and Wu (2017)]. A SINS error model under swaying base was constructed [Xiong, Peng, Wang et al. (2015)], analyzing the ship-board weapon self-initialization procedure [Wang, Shen and Ma (2008)] and proposed a new lever-arm compensation method under the base of traditional lever-arm compensation method. The novel method [Chen, Liu, Cheng et al. (2017); Fu, Huang, Ren et al. (2017)] was proved more accurate and with high precision with simulation experiments. An improved fast transfer alignment algorithm was proposed [Xia, Zhang and Lei (2017); Liu, Xu, Zhao et al. (2014)] and derived the construction method of velocity and z axis misalignment measurement [Fu, Wu, Wang et al. (2017); Sun and Gu (2017)]. The reduced-order transfer alignment filtering model [Guo, Xu and Li (2017); Hong, Lee, Chun et al. (2005)] was presented and the performance of the reduced order filtering model is validated by simulation.

The remainder of this paper is organized as follows: the description of novel initial alignment error models is presented in Section II. The Observability analysis of the transfer alignment is given in Section III. Simulation experiments are conducted and the simulation results are given in Section IV. The conclusion can be found in Section V.

Firstly, define relevant basic frames:

i frame-earth centered inertial frame;

e frame-earth centered earth fixed frame;

g frame-east-north-up geographic frame;

m frame-body frame of master INS;

s frame-body frame of slave INS;

Assuming that $L$ represents the latitude, $\lambda$ represents longitude, $\omega_{ie}$ is the earth rotation angular velocity, the local acceleration due to the actual gravity is denoted by g, $\phi$ is

defined as the misalignment angle. $(O_b X_b Y_b Z_b)$ stands for the body frame, $(O_e X_e Y_e Z_e)$ stands for the earth frame, $(O_n X_n Y_n Z_n)$ stands for the navigation frame, $(O_i X_i Y_i Z_i)$ represents the inertial frame. The subscripts b, e, i, n denote the corresponding components in each frame.

## 2 Error models

Suppose $(O_i X_i Y_i Z_i)$ represents the inertial frame, $(O_b X_b Y_b Z_b)$ stands for the body frame. $O_b$ is the swaying center of the ship, also is known as the gravitational center of the body.

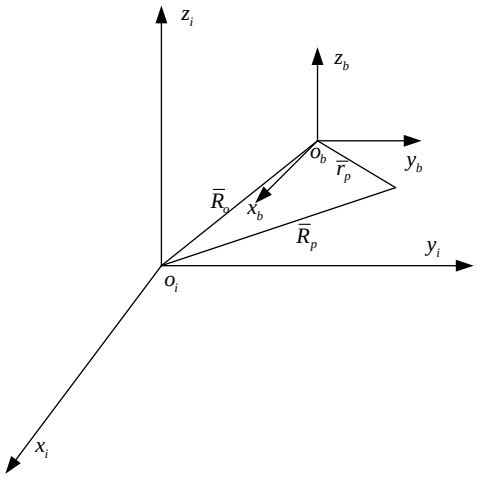


**Figure 1:** Lever arm effect sketch

The position of the center of gravity is calculated according to the general design of the load distribution, assuming that the gravity center is fixed and the master INS installation position is in coincidence with $O_b$, the slave INS accelerometer is fixed point P mounted on the carrier coordinates, position vector coordinate origin, P point position relative to the inertial coordinate vector at P, relative to the position vector vector coordinate origin. Obviously, they have the following relationship:

The position of the gravity center is usually calculated according to the load distribution of design, which is always fixed and coincides with the master inertial navigation system equipping position. The accelerometers of slave inertial navigation system are equipped at the fixed point p in the body frame. The position vector of the origin of the carrier coordinate system is $\overline{R}_0$, the position vector of p to inertial frame origin is $\overline{R}_p$, the position vector of p to the carrier frame origin is $\overline{r}_p$, abiding the following rules:

$$\overline{R}_p = \overline{R}_0 + \overline{r}_p \tag{1}$$

The differential of the upper formulae to time can be obtained:

$$\left.\frac{d\bar{R}_p}{dt}\right|_i = \left.\frac{d\bar{R}_0}{dt}\right|_i + \left.\frac{d\bar{r}_p}{dt}\right|_b + \bar{\omega}_{ib} \times \bar{r}_p \tag{2}$$

The differential of the upper formulae to time can be obtained:

$$\left.\frac{d^2\bar{R}_p}{dt^2}\right|_i = \left.\frac{d^2\bar{R}_0}{dt^2}\right|_i + \left.\frac{d}{dt}\left(\left.\frac{d\bar{r}_p}{dt}\right|_b\right)\right|_i + \left.\frac{d}{dt}(\bar{\omega}_{ib} \times \bar{r}_p)\right|_i \tag{3}$$

According to the relative micro quotient principle of vector differential, it can be obtained:

$$\left.\frac{d}{dt}\left(\left.\frac{d\bar{r}_p}{dt}\right|_b\right)\right|_i = \left.\frac{d^2\bar{r}_p}{dt^2}\right|_b + \bar{\omega}_{ib} \times \left.\frac{d\bar{r}_p}{dt}\right|_b \tag{4}$$

$\left.\frac{d^2\bar{r}_p}{dt^2}\right|_b$ presents linear acceleration of p to carrier frame.

The same reason can be obtained:

$$\begin{aligned}\left.\frac{d}{dt}(\bar{\omega}_{ib} \times \bar{r}_p)\right|_i &= \left.\frac{d\bar{\omega}_{ib}}{dt}\right|_i \times \bar{r}_p + \bar{\omega}_{ib} \times \left.\frac{d\bar{r}_p}{dt}\right|_i \\ &= \left.\frac{d\bar{\omega}_{ib}}{dt}\right|_i \times \bar{r} + \bar{\omega}_{ib} \times \left(\left.\frac{d\bar{r}_p}{dt}\right|_b + \bar{\omega}_{ib} \times \bar{r}_p\right) \\ &= \left.\frac{d\bar{\omega}_{ib}}{dt}\right|_i \times \bar{r} + \bar{\omega}_{ib} \times \left.\frac{d\bar{r}_p}{dt}\right|_b + \bar{\omega}_{ib} \times (\bar{\omega}_{ib} \times \bar{r}_p)\end{aligned} \tag{5}$$

The linear acceleration of p to inertial frame can be expressed as:

$$\left.\frac{d^2\bar{R}_p}{dt^2}\right|_i = \left.\frac{d^2\bar{R}_0}{dt^2}\right|_i + \left.\frac{d^2\bar{r}_p}{dt^2}\right|_b + 2\bar{\omega}_{ib} \times \left.\frac{d\bar{r}_p}{dt}\right|_b + \left.\frac{d\bar{\omega}_{ib}}{dt}\right|_i \times \bar{r}_p + \bar{\omega}_{ib} \times (\bar{\omega}_{ib} \times \bar{r}_p) \tag{6}$$

The carrier structure is rigid in the study of lever arm effect. Other methods are needed to compensate the error caused by the flexible deformation. P is fixed to the carrier frame here.

$$\left.\frac{d\bar{r}_p}{dt}\right|_b = 0, \quad \left.\frac{d^2\bar{r}_p}{dt^2}\right|_b = 0 \tag{7}$$

$$\left.\frac{d^2\bar{R}_p}{dt^2}\right|_i = \left.\frac{d^2\bar{R}_0}{dt^2}\right|_i + \left.\frac{d\bar{\omega}_{ib}}{dt}\right|_i \times \bar{r}_p + \bar{\omega}_{ib} \times (\bar{\omega}_{ib} \times \bar{r}_p) \tag{8}$$

The installation point should be in the swing center of the carrier in the ideal situation, $\bar{r}_p = 0$, the lever arm effect did not exist in the situation. The master inertial navigation is equipped at the carrier swing center, while the slave inertial navigation system cannot

satisfy the needs in transfer alignment. Lever arm effect cannot be neglected in real application. The latter two components are caused by the lever arm effect, sensed by the slave inertial navigation system, not sensed by the master inertial navigation system. $\delta \overline{f}$ stands for the lever arm acceleration, the standard equation of the lever arm effect error is,

$$\delta \overline{f} = \left.\frac{d\overline{\omega}_{ib}}{dt}\right|_i \times \overline{r}_p + \overline{\omega}_{ib} \times (\overline{\omega}_{ib} \times \overline{r}_p) \tag{9}$$

For

$$\left.\frac{d\overline{\omega}_{ib}}{dt}\right|_i = \left.\frac{d\overline{\omega}_{ib}}{dt}\right|_b + \overline{\omega}_{ib} \times \overline{\omega}_{ib} \tag{10}$$

$$\begin{aligned} \delta \overline{f} &= (\left.\frac{d\overline{\omega}_{ib}}{dt}\right|_b + \overline{\omega}_{ib} \times \overline{\omega}_{ib}) \times \overline{r}_p + \overline{\omega}_{ib} \times (\overline{\omega}_{ib} \times \overline{r}_p) \\ &= \left.\frac{d\overline{\omega}_{ib}}{dt}\right|_b \times \overline{r}_p + 2\overline{\omega}_{ib} \times (\overline{\omega}_{ib} \times \overline{r}_p) \end{aligned} \tag{11}$$

While $\left.\frac{d\overline{\omega}_{ib}}{dt}\right|_b \times \overline{r}_p$ stands for the tangential acceleration, $\overline{\omega}_{ib} \times (\overline{\omega}_{ib} \times \overline{r}_p)$ stands for the centripetal acceleration.

The swing angle rate and angle rate differential in the carrier frame to the navigation frame are as follows,

$$\overline{\omega}_{nb}^b = \begin{bmatrix} -\dot{\psi}\sin\gamma\sin\theta + \dot{\gamma}\cos\gamma \\ \dot{\psi}\sin\theta + \dot{\gamma} \\ \dot{\psi}\cos\gamma\cos\theta + \dot{\theta}\sin\gamma \end{bmatrix} \tag{12}$$

$$\dot{\overline{\omega}}_{nb}^b = \begin{bmatrix} -\ddot{\psi}\sin\gamma\sin\theta + \ddot{\gamma}\cos\gamma \\ \ddot{\psi}\sin\theta + \ddot{\gamma} \\ \ddot{\psi}\cos\gamma\cos\theta + \ddot{\theta}\sin\gamma \end{bmatrix} \tag{13}$$

For

$$\overline{\omega}_{ib}^n = \overline{\omega}_{ie}^n + \overline{\omega}_{en}^n + \overline{\omega}_{nb}^n = \overline{\omega}_{ie}^n + \overline{\omega}_{en}^n + C_b^n \overline{\omega}_{nb}^b \tag{14}$$

Suppose the vehicle did not move linearly, that is $\overline{\omega}_{en}^n = \begin{bmatrix} 0 & 0 & 0 \end{bmatrix}^T$, the above formulae can be simplified as

$$\overline{\omega}_{ib}^n = \overline{\omega}_{ie}^n + C_b^n \overline{\omega}_{nb}^b \tag{15}$$

$$\dot{\overline{\omega}}_{ib}^n = \dot{\overline{\omega}}_{ie}^n + \dot{\overline{\omega}}_{en}^n + \dot{\overline{\omega}}_{nb}^n = C_b^n \dot{\overline{\omega}}_{nb}^b \tag{16}$$

The lever arm effect acceleration can be expressed in the navigation frame as follows

$$\begin{aligned}\delta \overline{f}^n &= C_b^n \dot{\overline{\omega}}_{nb}^b \times \overline{r}_p + (\overline{\omega}_{ie}^n + C_b^n \overline{\omega}_{nb}^b) \times (\overline{\omega}_{ie}^n + C_b^n \overline{\omega}_{nb}^b) \times \overline{r}_p \\ &= C_b^n \dot{\overline{\omega}}_{nb}^b \times \overline{r}_p + \overline{\omega}_{ie}^n \times (\overline{\omega}_{ie}^n \times \overline{r}_p) + \overline{\omega}_{ie}^n \times \left[ (C_b^n \overline{\omega}_{nb}^b) \times \overline{r}_p \right] \\ &+ (C_b^n \overline{\omega}_{nb}^b) \times (\overline{\omega}_{ie}^n \times \overline{r}_p) + (C_b^n \overline{\omega}_{nb}^b) \times [(C_b^n \overline{\omega}_{nb}^b) \times \overline{r}_p]\end{aligned} \tag{17}$$

Suppose

$$\delta \overline{f}_1^n = 2\overline{\omega}_{ie}^n \times \overline{\omega}_{ie}^n \times \overline{r}_p \tag{18}$$

$$\delta \overline{f}_2^n = C_b^n \dot{\overline{\omega}}_{nb}^b \times \overline{r}_p \tag{19}$$

$$\delta \overline{f}_3^n = \overline{\omega}_{ie}^n \times \left[ (C_b^n \overline{\omega}_{nb}^b) \times \overline{r}_p \right] \tag{20}$$

$$\delta \overline{f}_4^n = (C_b^n \overline{\omega}_{nb}^b) \times (\overline{\omega}_{ie}^n \times \overline{r}_p) \tag{21}$$

$$\delta \overline{f}_5^n = (C_b^n \overline{\omega}_{nb}^b) \times [(C_b^n \overline{\omega}_{nb}^b) \times \overline{r}_p] \tag{22}$$

while $\delta \overline{f}_1^n = 2\overline{\omega}_{ie}^n \times \overline{\omega}_{ie}^n \times \overline{r}_p$ presents the constant component caused by the earth rotation.

Suppose

$$r_p^n = \begin{bmatrix} r_x \\ r_y \\ r_z \end{bmatrix}, \quad C_b^n = \begin{bmatrix} c_{11} & c_{12} & c_{13} \\ c_{21} & c_{22} & c_{23} \\ c_{31} & c_{32} & c_{33} \end{bmatrix} \tag{23}$$

And for

$$\overline{\omega}_{ie}^n = \begin{bmatrix} \omega_{iex} \\ \omega_{iey} \\ \omega_{iez} \end{bmatrix} = \begin{bmatrix} 0 \\ \omega_{ie} \cos\varphi \\ \omega_{ie} \sin\varphi \end{bmatrix} \tag{24}$$

Can be derived that

$$\delta \overline{f}_2^n = \begin{bmatrix} (c_{21} r_z - c_{31} r_y) \dot{\omega}_{nbx}^b + (c_{22} r_z - c_{32} r_y) \dot{\omega}_{nby}^b + (c_{23} r_z - c_{33} r_y) \dot{\omega}_{nbz}^b \\ (c_{31} r_x - c_{11} r_z) \dot{\omega}_{nbx}^b + (c_{32} r_z - c_{12} r_y) \dot{\omega}_{nby}^b + (c_{33} r_z - c_{13} r_y) \dot{\omega}_{nbz}^b \\ (c_{11} r_x - c_{21} r_z) \dot{\omega}_{nbx}^b + (c_{12} r_z - c_{22} r_y) \dot{\omega}_{nby}^b + (c_{13} r_z - c_{23} r_y) \dot{\omega}_{nbz}^b \end{bmatrix} \tag{25}$$

$$\delta \overline{f}_3^n = \overline{\omega}_{ie}^n \times \left[ \left( C_b^n \overline{\omega}_{nb}^b \right) \times \overline{r}_p \right] = \begin{bmatrix} (r_z \omega_{iez} + r_y \omega_{iey}) \omega_{nbx}^b - r_x \omega_{iey} \omega_{nby}^b + r_x \omega_{iez} \omega_{nbz}^b \\ -r_y \omega_{iex} \omega_{nbx}^b + (r_z \omega_{iez} + r_x \omega_{iex}) \omega_{nby}^b - r_y \omega_{iez} \omega_{nbz}^b \\ -r_z \omega_{iex} \omega_{nbx}^b - r_z \omega_{iey} \omega_{nby}^b + (r_y \omega_{iey} + r_x \omega_{iex}) \omega_{nbz}^b \end{bmatrix} \tag{26}$$

$$\delta \overline{f}_4^n = \left(C_b^n \overline{\omega}_{nb}^b\right) \times \left(\overline{\omega}_{ie}^n \times \overline{r}_p\right)$$

$$= \begin{bmatrix} [(\omega_{iex} r_y - \omega_{iey} r_x) c_{21} + (\omega_{iex} r_z - \omega_{iez} r_x) c_{31}] \omega_{nbx}^b + [(\omega_{iex} r_y - \omega_{iey} r_x) c_{22} \\ [(\omega_{iey} r_z - \omega_{iez} r_y) c_{11} + (\omega_{iey} r_z - \omega_{iez} r_z) c_{31}] \omega_{nbx}^b + [(\omega_{iey} r_z - \omega_{iez} r_y) c_{12} \\ [(\omega_{iez} r_x - \omega_{iex} r_z) c_{11} + (\omega_{iez} r_y - \omega_{iey} r_z) c_{21}] \omega_{nbx}^b + [(\omega_{iez} r_x - \omega_{iex} r_z) c_{12} \end{bmatrix} \quad (27)$$

$$\begin{bmatrix} +(\omega_{iex} r_z - \omega_{iez} r_x) c_{32}] \omega_{nby}^b + [(\omega_{iex} r_y - \omega_{iey} r_x) c_{23} + (\omega_{iex} r_z - \omega_{iez} r_x) c_{33}] \omega_{nbz}^b \\ +(\omega_{iey} r_z - \omega_{iez} r_y) c_{32}] \omega_{nby}^b + [(\omega_{iey} r_z - \omega_{iez} r_y) c_{13} + (\omega_{iey} r_z - \omega_{iez} r_y) c_{33}] \omega_{nbz}^b \\ +(\omega_{iez} r_y - \omega_{iey} r_z) c_{22}] \omega_{nby}^b + [(\omega_{iez} r_x - \omega_{iex} r_z) c_{13} + (\omega_{iez} r_y - \omega_{iey} r_z) c_{23}] \omega_{nbz}^b \end{bmatrix}$$

$$\delta \overline{f}_5^n = \left(C_b^n \overline{\omega}_{nb}^b\right) \times \left[\left(C_b^n \overline{\omega}_{nb}^b\right) \times \overline{r}_p\right]$$

$$= \begin{bmatrix} (c_{21}\omega_{nbx}^b + c_{22}\omega_{nby}^b + c_{23}\omega_{nbz}^b)(c_{11}\omega_{nbx}^b + c_{12}\omega_{nby}^b + c_{13}\omega_{nbz}^b) r_y \\ (c_{11}\omega_{nbx}^b + c_{12}\omega_{nby}^b + c_{13}\omega_{nbz}^b)(c_{21}\omega_{nbx}^b + c_{22}\omega_{nby}^b + c_{23}\omega_{nbz}^b) r_x \\ (c_{11}\omega_{nbx}^b + c_{12}\omega_{nby}^b + c_{13}\omega_{nbz}^b)(c_{31}\omega_{nbx}^b + c_{32}\omega_{nby}^b + c_{33}\omega_{nbz}^b) r_x \end{bmatrix}$$

$$\begin{bmatrix} +(c_{31}\omega_{nbx}^b + c_{32}\omega_{nby}^b + c_{33}\omega_{nbz}^b)(c_{11}\omega_{nbx}^b + c_{12}\omega_{nby}^b + c_{13}\omega_{nbz}^b) r_z \\ +(c_{31}\omega_{nbx}^b + c_{32}\omega_{nby}^b + c_{33}\omega_{nbz}^b)(c_{21}\omega_{nbx}^b + c_{22}\omega_{nby}^b + c_{23}\omega_{nbz}^b) r_z \\ +(c_{21}\omega_{nbx}^b + c_{22}\omega_{nby}^b + c_{23}\omega_{nbz}^b)(c_{31}\omega_{nbx}^b + c_{32}\omega_{nby}^b + c_{33}\omega_{nbz}^b) r_y \end{bmatrix} \quad (28)$$

$$\begin{bmatrix} -[(c_{21}\omega_{nbx}^b + c_{22}\omega_{nby}^b + c_{23}\omega_{nbz}^b)^2 + (c_{31}\omega_{nbx}^b + c_{32}\omega_{nby}^b + c_{33}\omega_{nbz}^b)^2] r_x \\ -[(c_{11}\omega_{nbx}^b + c_{12}\omega_{nby}^b + c_{13}\omega_{nbz}^b)^2 + (c_{31}\omega_{nbx}^b + c_{32}\omega_{nby}^b + c_{33}\omega_{nbz}^b)^2] r_y \\ -[(c_{11}\omega_{nbx}^b + c_{12}\omega_{nby}^b + c_{13}\omega_{nbz}^b)^2 + (c_{21}\omega_{nbx}^b + c_{22}\omega_{nby}^b + c_{23}\omega_{nbz}^b)^2] r_z \end{bmatrix}$$

## 3 Observability analysis

Before AUV entering the water, transfer alignment is conducted before integrated navigation period. Transfer alignment uses the navigation information of position, velocity and attitude from master inertial navigation system equipped on the big ship. Observability analysis was conducted on the SINS state vector based on SVD method. State equation of SINS was adopted as the system state equation. Observability analysis was conducted under different vehicle motion with SINS/DVL integration and different matching methods under three-axis swaying mode.

Suppose the vehicle was navigating at a certain depth, the navigation velocity was 10 m/s, navigation depth was 20 meters. The initial latitude $L = 32^\circ$ the initial longitude $\lambda = 118^\circ$, the gyro constant drift was $1^\circ/h$, the gyro random drift was $1^\circ/h$, the accelerometer constant drift was $50\,\mu g$, the accelerometer random drift was $50\,\mu g$, sampling time was 1 s.

Observability analyses of velocity matching were conducted under different vehicle motions. Simulation experiments were conducted under stationary base, dual-axis swaying, three-axis swaying, acceleration and turning motion with velocity matching.

The measurement information is the vehicle velocity (north velocity and east velocity) and velocity from the master inertial navigation system.

The motion process of initial alignment on moving base can be designed as follows, the gyro drift is estimated under three-axis swaying and linear acceleration. The accelerometer bias is estimated under linear acceleration and turning, the angle error can be estimated under linear constant navigation.

The observability degree of the state variables under three-axis swaying with velocity, heading angle error and position matching is presented in Tab. 1.

**Table 1:** Observability degree under three-axis swaying with velocity, heading angle error and position matching

| State Variable | East Velocity Error | North Velocity Error | East Angle Error | North Angle Error | Up Angle Error | Latitude Error |
|---|---|---|---|---|---|---|
| 1st time period | 1.0 | 1.0 | 10.1752 | 9.8386 | 0.96692 | 1.0 |
| 2nd time period | 1.0 | 1.0 | 9.8388 | 10.1727 | 0.9678 | 1.0 |
| 3rd time period | 1.0 | 1.0 | 9.8385 | 10.1668 | 0.9698 | 1.0 |
| State Variable | Longitude Error | East Acc Bias | North Acc Bias | East Gyro Drift | North Gyro Drift | Up Gyro Drift |
| 1st time period | 1.0 | 0 | 0 | 9.7876 | 10.1259 | 0.9666 |
| 2nd time period | 1.0 | 0.0141 | 0.0139 | 9.7874 | 10.1228 | 0.9801 |
| 3rd time period | 1.0 | 0.0230 | 0.0226 | 9.7856 | 10.1155 | 1.0033 |

From Tab. 1, eastern velocity error, northern velocity error, up heading angle error, longitude error, latitude error, eastern gyro drift, northern gyro drift, up gyro drift are high in observability degree and the filter effects are good. Eastern accelerometer bias and northern accelerometer bias are low in observability degree and the filter effects are not good.

From the analysis above, the velocity error can be well estimated with velocity matching while heading angle and position error cannot be well estimated. The heading angle error can be better estimated with velocity and heading matching, while the position error cannot be well estimated. The heading angle error, velocity error, position error can be well estimated with velocity, heading and position matching.

## 4 Revised lever-arm effect compensation method

When the ship is under mooring condition, the linear acceleration and the linear velocity is zero, the error equation of the inertial system can be reduced as follows,

$$\begin{cases} \delta\dot{V}^{n'} = g^{n'} \times \phi - 2\omega_{ie}^{n'} \times \delta V^{n'} + C_b^{n'} \delta f^b + C_b^{n'} \nabla^b \\ \dot{\phi} = -\omega_{ie}^{n'} \times \phi + \delta\omega_{ie}^{n'} + C_b^{n'} \varepsilon^b \\ \dot{\nabla}^b = 0, \dot{\varepsilon}^b = 0, \dot{r}^b = 0 \end{cases} \tag{29}$$

$n'$ is the navigation frame, b is the body frame, $\delta V$ is the body velocity error, $\phi$ is the vehicle attitude error, $\omega_{ie}^{n'}$ is the earth rotation rate on the navigation frame, $\delta\omega_{ie}^{n'}$ is the computational error, $g^{n'}$ is the gravitational acceleration on the navigation frame. $\delta f^b$ is the lever arm acceleration, $\nabla^b$ is the acceleration constant drift, $\varepsilon^b$ is the gyro constant drift, $r^b$ is the lever arm length on the body frame, $C_b^{n'}$ is the strapdown matrix.

In the strapdown inertial navigation system, Kalman filter is applied in the estimation of lever arm length. The accelerometer error and the gyro drift gyro are expanded as the states in the Kalman filter. The system state equation is as follows,

$$\dot{X} = AX + BW \tag{30}$$

State variables and the noise vector are as follows,

$$X = \begin{bmatrix} \delta V_e & \delta V_n & \phi_e & \phi_n & \phi_u & \nabla_x & \nabla_y & \varepsilon_x & \varepsilon_y & \varepsilon_z & r_x & r_y & r_z \end{bmatrix}^T$$

$$W = \begin{bmatrix} a_x & a_y & \omega_x & \omega_y & \omega_z & 0 & 0 & 0 & 0 & 0 & 0 & 0 & 0 \end{bmatrix}^T$$

Coefficient matrix

$$A = \begin{bmatrix} A_{11} & A_{12} & C_{2\times2} & 0_{2\times3} & A_{15} \\ A_{21} & A_{22} & 0_{2\times2} & C_b^{n'} & 0_{3\times3} \\ 0_{8\times2} & 0_{8\times3} & 0_{8\times2} & 0_{8\times3} & 0_{8\times3} \end{bmatrix}$$

$$A_{11} = \begin{bmatrix} 0 & 2\omega_{ie}\sin\varphi \\ -2\omega_{ie}\sin\varphi & 0 \end{bmatrix}$$

$$A_{12} = \begin{bmatrix} 0 & -g & 0 \\ g & 0 & 0 \end{bmatrix}$$

$$A_{21} = \begin{bmatrix} 0 & -1/R_e \\ 1/R_e & 0 \\ \tan\varphi/R_e & 0 \end{bmatrix}$$

$$A_{22} = \begin{bmatrix} 0 & \omega_{ie}\sin\varphi & -\omega_{ie}\cos\varphi \\ -\omega_{ie}\sin\varphi & 0 & 0 \\ \omega_{ie}\cos\varphi & 0 & 0 \end{bmatrix}$$

$$A_{15} = \begin{bmatrix} -\left(\omega_n^2 + \omega_u^2\right) & \omega_e\omega_n - \dot{\omega}_u & \omega_n\omega_u + \dot{\omega}_n \\ \omega_e\omega_n + \dot{\omega}_u & -\left(\omega_e^2 + \omega_u^2\right) & \omega_u\omega_n - \dot{\omega}_e \end{bmatrix}$$

$$B=\begin{bmatrix} C_{2\times2} & 0_{2\times3} & 0_{2\times8} \\ 0_{3\times2} & C_b^{n'} & 0_{3\times8} \\ 0_{8\times2} & 0_{8\times3} & 0_{8\times8} \end{bmatrix} C_b^{n'}=\begin{bmatrix} C_{11} & C_{12} & C_{13} \\ C_{21} & C_{22} & C_{23} \\ C_{31} & C_{32} & C_{33} \end{bmatrix} C_{2\times2}=\begin{bmatrix} C_{11} & C_{12} \\ C_{21} & C_{22} \end{bmatrix}$$

$\varphi$ is the latitude, $R_e$ is the earth radius, $\omega_{ib}^b=\begin{bmatrix}\omega_e & \omega_n & \omega_u\end{bmatrix}^T$ is the gyro angle velocity, $\dot{\omega}_{ib}^b=\begin{bmatrix}\dot{\omega}_e & \dot{\omega}_n & \dot{\omega}_u\end{bmatrix}^T$ is the angle acceleration.

The measurement variable is $\delta V_e$ and $\delta V_n$, the measurement equation is

$$Z=HX \tag{31}$$

$Z=\begin{bmatrix}\delta V_e & \delta V_n\end{bmatrix}^T$ is the observation vector, the measurement vector is $H=\begin{bmatrix}I_{2\times2} & 0_{2\times11}\end{bmatrix}$

## 5 Simulation and results

In the simulation experiments, the performance of each transfer alignment algorithm is evaluated. The ship speed is about 30knots. The angular motions of the ship are generated as follows

Suppose the initial longitude is 118°, the initial latitude is 32°, the initial height is 0. The initial longitude error is 5'', the initial latitude error is 5'', and the initial height error is 5''. The initial eastern velocity is 10m/s, the initial northern velocity is 10m/s, the initial eastern velocity error is 0.1m/s, the initial northern velocity is 0.1m/s, the initial heading $H_0$ is 45°, the initial pitching angle is 0°, the initial rolling angle is 0°. Initial heading, pitching and rolling angle error is $10'',10'',30''$ respectively. Accelerometer constant drift and random drift is 100ug. The gyro constant drift and random drift is 0.1°/h. The swing amplitude of heading, pitching and rolling is 14°, 9°and 12° respectively. The swing period of heading, pitching and rolling is 6 s, 8 s, and 10 s respectively. The ship swing model which is suffering the wind and tide under the mooring condition is as follows,

$$\begin{cases} P=P_m\sin(2\pi/T_P+\phi_P) \\ R=R_m\sin(2\pi/T_R+\phi_R) \\ H=H_m\sin(2\pi/T_H+\phi_H)+H_0 \end{cases} \tag{32}$$

The lever arm length is $\begin{bmatrix}2m & 2m & 1m\end{bmatrix}^T$, DVL velocity error is 0.1 m/s, the DVL error coefficient is 0.0001.

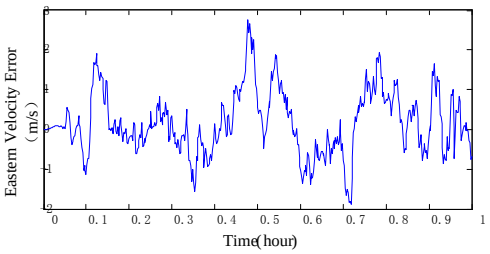


(a): Eastern velocity error (0-1 h)

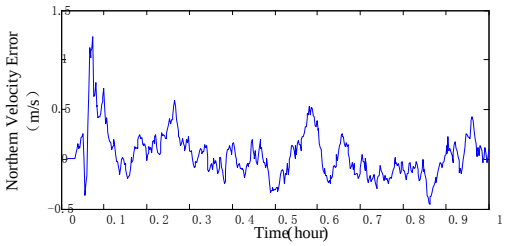


(b): Northern velocity error (0-1 h)

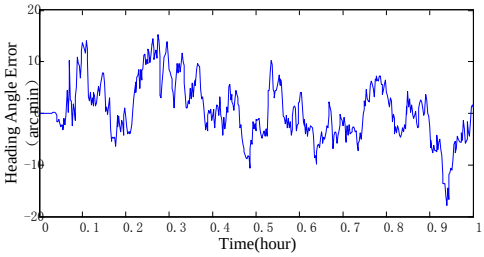


(c): Heading angle error (0-1 h)

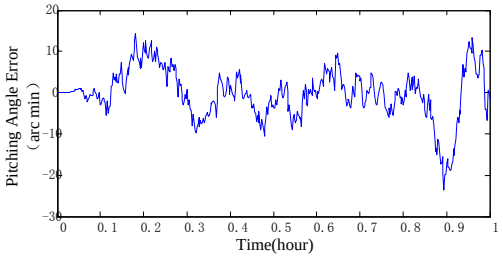


(d): Pitching angle error (0-1 h)

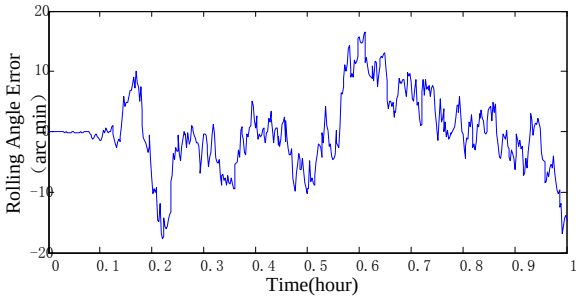


(e): Rolling angle error (0-1 h)

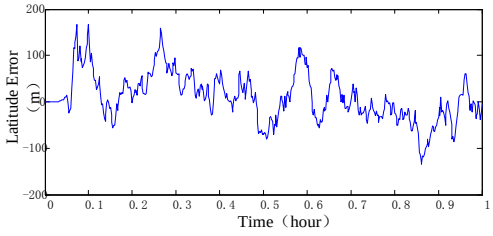


(f): Latitude error (0-1 h)

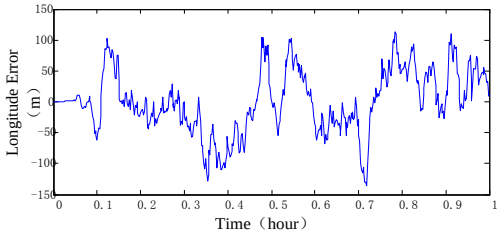


(g): Longitude error (0-1 h)

**Figure 2:** Navigation error of the integrated navigation without lever arm compensation

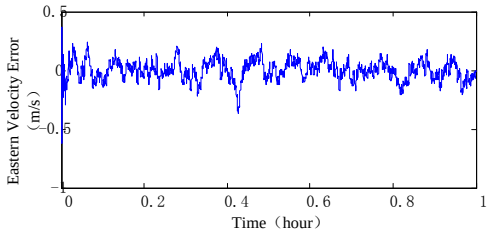


(a): Easter velocity error (0-1 h)

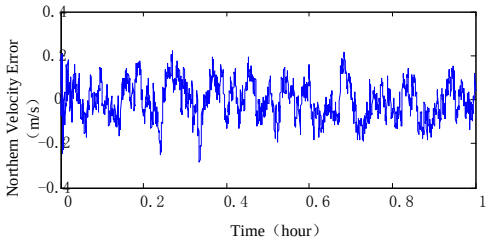


(b): Northern velocity error (0-1 h)

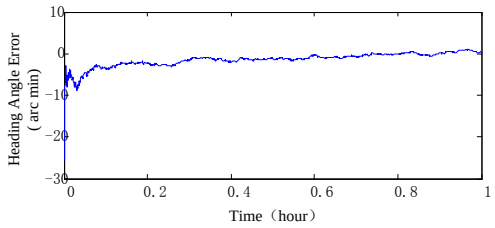


(c): Heading angle error (0-1 h)

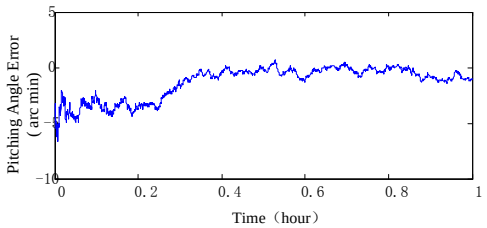


(d): Pitching angle error (0-1 h)

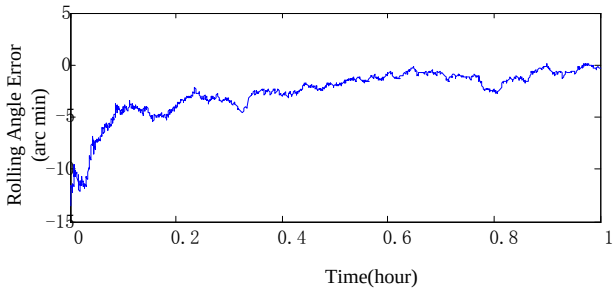


(e): Rolling angle error (0-1 h)

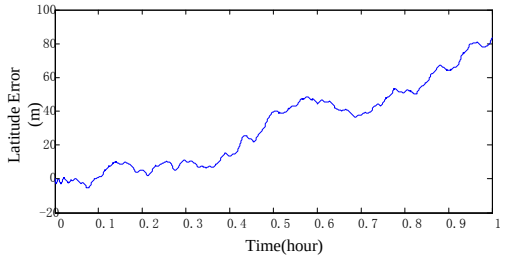


(f): Latitude error (0-1 h)

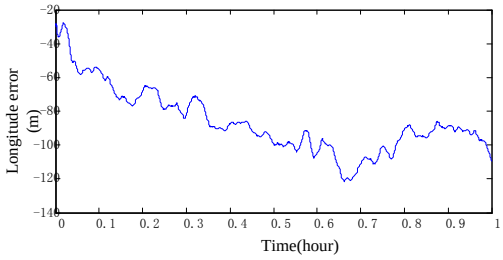


(g): Longitude error (0-1 h)

**Figure 3:** Navigation error of the integrated navigation with lever arm compensation

## 6 Conclusions

This paper presents an efficient transfer alignment approach for swaying base big ship navigation system. A novel algorithm associated with the transfer alignment is employed

to obtain the mathematical platform for the navigation system. Considering the environmental disturbances and the sensor drift as the main error source, a nonlinear filter approach is applied to the system to reduce the lever arm effect on the acceleration measurement. Observability analysis is conducted to different vehicle motion. Simulation experiments were conducted and the results showed that the novel method is able to improve the rapidity and precision of transfer alignment, overcoming the lever arm effect and disturbances existing in the host inertial navigation system and the slave inertial navigation system in the application of big ship navigation initial alignment.

**Acknowledgement:** This work is funded by Natural Science Foundation of Jiangsu Province under Grant BK20160955, a project funded by the Priority Academic Program Development of Jiangsu Higher Education Institutions and Science Research Foundation of Nanjing University of Information Science and Technology under Grant 20110430. Open Foundation of Jiangsu Key Laboratory of Meteorological Observation and Information Processing (KDXS1304), Open Foundation of Jiangsu Key Laboratory of Ocean Dynamic Remote Sensing and Acoustics (KHYS1405).

**References**

**Chen, H.; Liu, J.; Cheng, X.; Liu, N.** (2017): Design and stability analysis of robot SGQKF transfer alignment filter for incomplete measurement system with stochastic disturbance. *Journal of Chinese Inertial Technology*, vol. 25, no. 4, pp. 171-181.

**Chen, X.; Chen, S.; Wu, Y.** (2017): Coverless information hiding method based on the Chinese character encoding. *Journal of Internet Technology*, vol. 18, no. 2, pp. 313-320.

**Cheng, X.; Wang, X.; Liu, F.** (2014): The application of sparse grid quadrature filter on SINS/GPS tightly coupled integration. *Journal of Chinese Inertial Technology*, vol. 22, no. 6, pp. 799-804.

**Fu, Z.; Huang, F.; Ren, K.; Weng, J.; Wang, C.** (2017): Privacy-preserving smart semantic search based on conceptual graphs over encrypted outsourced data. *IEEE Transactions on Information Forensics and Security*, vol. 12, no. 8, pp. 1874-1884.

**Fu, Z.; Wu, X.; Wang, Q.; Ren, K.** (2017): Enabling central keyword-based semantic extension search over encrypted outsourced data. *IEEE Transactions on Information Forensics and Security*, vol. 12, no. 12, pp. 2986-2997.

**Guo, S.; Xu, J.; Li, F.** (2017): Strong tracking cubature Kalman filter for initial alignment of inertial navigation system. *Journal of Chinese Inertial Technology*, vol. 25, no. 4, pp. 436-441.

**Hong, S.; Lee, M.; Chun, H.; Kwon, S.; Speyer, J.** (2005): Observability of error states in GPS/INS Integration. *IEEE Transactions on vehicular technology*, vol. 54, no. 2, pp. 731-743.

**John, B.; Leondes, C.** (1972): In-flight alignment and calibration of inertial measurement unit-part I: general formulation. *IEEE Transactions on Aerospace and Electronic System*, vol. 8, no. 4, pp. 439-449.

**Kassas, Z.; Humphreys, T.** (2014): Observability analysis of collaborative opportunistic navigation with pseudorange measurements. *IEEE Transactions on Intelligent Transportation Systems*, vol. 15, no. 1, pp. 260-273.

**Li, S.; Wang, Y.; Liu, Z.** (2014): Comparison of wing distortion estimation methods in transfer alignment. *Journal of Chinese Inertial Technology*, vol. 22, no. 1, pp. 38-44.

**Liu, X.; Xu, X.; Zhao, Y.; Wang, L.; Liu, Y.** (2014): An initial alignment method for strapdown gyrocompass based on gravitational apparent motion in inertial frame. *Measurement*, vol. 55, no. 6, pp. 593-604.

**Sun, Y.; Gu, F.** (2017): Compressive sensing of piezoelectric sensor response signal for phased array structural health monitoring. *International Journal of Sensor Networks*, vol. 23, no. 4, pp. 258-264.

**Sun, J.; Xu, X; Liu, Y.** (2016): Initial alignment of large azimuth misalignment in SINS based on adaptive unscented particle filter. *Journal of Chinese Inertial Technology*, vol. 24, no. 2, pp. 154-159.

**Wang, B.; Gu, X.; Ma, L.; Yan, S.** (2017): Temperature error correction based on BP neural network in meteorological WSN. *International Journal of Sensor Networks*, vol. 23, no. 4, pp. 265-278.

**Wang, X.; Shen, L.; Ma, S.** (2008): Transfer alignment of strapdown inertial navigation system on rolling bases. *Journal of Beijing University of Aeronautics and Astronautics*, vol. 35, no. 6, pp. 728-731.

**Xia, J.; Zhang, J.; Lei, H.** (2017): Improved velocity plus attitude matching fast transfer alignment algorithm. *Journal of Chinese Inertial Technology*, vol. 25, no. 1, pp. 17-21.

**Xiong, Z.; Peng, H.; Wang, J; Wang, R; Liu, J.** (2015): Dynamic calibration method for SINS lever-arm effect for HCVs. *IEEE Transactions on Aerospace and Electronic Systems*, vol. 51, no. 4, pp. 2760-2771.

**Xu, X.; Wan, D.** (1994): Research on the lever-arm error in the shipboard strapdown inertial navigation system. *Journal of Southeast University*, vol. 24, no. 2, pp. 122-126.

**Zhou, Z.; Wang, Y.; Wu, J.; Yang, C. Sun, X.** (2017): Effective and efficient global context verification for image copy detection. *IEEE Transactions on Information Forensics and Security*, vol. 12, no. 1, pp. 48-63.

**Zhu, L.; Cheng, X.** (2013): An improved initial alignment method for rocket navigation system. *Journal of Navigation*, vol. 66, no. 5, pp. 737-749.

**Zhu, Y.; Cheng, X.; Wang, L.** (2016): A novel fault detection method for an integrated navigation system using Gaussian process regression. *Journal of Navigation*, vol. 69, no. 4, pp. 905-919.